

Supporting Information

Braver et al. 10.1073/pnas.0808187106

SI Methods

Participants. Participants were neurologically normal, right-handed younger or older adults. The groups did not differ in gender breakdown ($X^2 = 1.25$, $df = 1$, $n = 32$, $P = 0.26$). All participants gave informed consent per guidelines set by the Washington University Medical Center Human Studies Committee and were paid \$25 for each hour of participation in the fMRI study. Participants were screened for any signs of medical disorders (including treated or untreated hypertension, diabetes, and thyroid problems), neurological disorders (including past head injuries involving loss of consciousness for 5 or more minutes or a documented concussion), psychiatric disorders, medication histories that could influence cognitive performance, or any other contraindication for MR scanning. Older adults were administered the Blessed Orientation-Memory-Concentration Test (1) over the telephone. Individuals obtaining 5 or more errors were not included.

AX-CPT Task. Stimuli were single letters presented in white 36-point uppercase bold Helvetica font on a black screen. Presentation of an “X” probe required a target response (button press with index finger), but only if it was preceded by an “A” cue (AX trials). All other stimuli required nontarget responses (middle finger button press). Nontarget trials consist of 3 types: AY, BX, and BY, where B and Y refer to non-A cues and non-X probes. Trials were 7.5 s in duration and comprised the following events: cue (300 msec), delay (4,900 msec), probe (300 msec), response window (1,300 msec from probe onset), and visual feedback (1,000 msec; “Trial over, get ready for the next one.”).

Procedure: Older Adults. Following the baseline scanning session, older adult participants returned for a second session at least 1 week later. The first component of this session consisted of behavioral strategy training, following a protocol developed in ref. 2. Strategy training consisted of 3 phases: initial practice, strategy description, and incremental strategy practice. The strategy involved attending to classification of the cue (“A” vs. “not A”), followed by overt verbal classification, then translation of cue category to response rule (i.e., if cue = A, then use rule “if X, target”), with both overt and, then later, covert rehearsal of this rule during the delay period. The strategy training occurred over short 10-trial blocks and consisted of 80 trials total of strategy practice. Following the strategy training component (which lasted about 0.5 h), participants took a rest break and then immediately entered the fMRI scanner. The imaging component of the session consisted of scans during which the AX-CPT was performed according to the exact procedure followed in the first session: 2 task blocks of 20 trials each performed in each of 3 scanning runs, leading to a total of 120 AX-CPT trials performed (84 AX, 12 AY, 12 BX, 12 BY).

Procedure: Younger Adults. Following an initial baseline scanning session, younger adults underwent a second session (conducted on the same day, without leaving the scanner), in which the task was performed again under penalty incentive conditions. In this condition, before the start of each scanning run, participants were informed that a set of nogo trials (indicated via an underline bar beneath the probe) were added to the standard set of AX-CPT trials. Responses were to be withheld on these nogo trials, with each nogo error (failure to withhold responding) resulting in a \$3 penalty subtracted from their final payment. Nogo trials occurred with low (20%) frequency and were

randomly intermixed with standard AX-CPT trials (i.e., unpredictable until probe onset). Each time a nogo error occurred it was followed by a visual feedback message presented after the response (“You lost \$3!”) instead of the standard feedback message. The penalty incentive AX-CPT condition was performed in 3 scanning runs, with 40 AX-CPT trials performed in each scan in two 20-trial blocks (120 trials total; 60 AX, 12 AY, 12 BX, 12 BY, 24 nogo). With the exception of these changes, the task and procedure was identical to that of the standard AX-CPT performed in the first session.

Functional MRI Acquisition. Images were acquired on a Siemens 1.5 Tesla Vision System with a standard circularly polarized head coil. A pillow and tape were used to minimize head movement. Functional images were acquired using an asymmetric spin-echo echo-planar sequence (TR = 2,500 ms, TE = 50 ms, flip = 90°). Each image consisted of 18 contiguous, 7-mm-thick axial images (3.75 × 3.75 mm in plane) acquired parallel to the anterior-posterior commissure. High-resolution (1.25 × 1 × 1 mm) structural images were also acquired using a sagittal MP-RAGE 3D T1-weighted sequence (TR = 9.7 ms, TE = 4 ms, flip = 12°, TI = 300 ms).

Behavioral Data Analyses. Accuracy (percentage correct) and median reaction time (RT) data were computed for each of the 4 trial types (AX, AY, BX, and BY). An additional composite measure was created using the 2 trial types (AY, BX) that are the most salient measures of different aspects of context processing ability (8, 9). This proactive behavioral shift index was computed as $(AY - BX)/(AY + BX)$. The index was calculated for errors, RTs, and the sum of errors and RTs. A correction was made for trials where errors were equal to zero such that $(error + 0.5)/(frequency of trials + 1)$.

fMRI Analyses. Functional imaging data were preprocessed by correcting for movement and registered to the participant’s anatomical images. Event-related effects were analyzed with general linear models (GLMs) for each participant, estimating values for the time points with an unassumed shape for the hemodynamic response function. This GLM approach involved estimation of a 25-s (10 TR) event-related epoch for each trial type. Parameter estimates from each participant’s GLM were submitted to second-level tests treating participant as a random factor in *t* tests and ANOVAs.

To conclude that a previously identified ROI demonstrated a training-related proactive shift in older adults, the following criteria were used: (i) numerically greater cue activation in the posttest session compared with baseline, (ii) numerically greater probe activation in the baseline session compared with posttest, and (iii) a significant ($P < 0.05$) session (baseline vs. posttest) by event (cue vs. probe) interaction. To conclude that a previously identified ROI demonstrated a penalty-related reactive shift in younger adults, the following criteria were used: (i) numerically greater cue activation in the baseline condition compared with the penalty condition, (ii) numerically greater probe activation in the penalty condition compared with the baseline condition, and (iii) a significant ($P < 0.05$) session (baseline vs. penalty) by event (cue vs. probe) interaction. In all analyses, we defined cue/delay activity as the sum of activation at time points 3 and 4 (i.e., corresponding to 5–7.5 s after trial onset, which accommodates the well-known hemodynamic lag) and probe activity as

the sum of activation at time points 5 and 6 (i.e., corresponding to 10–12.5 s after trial onset).

Results

Behavioral Analyses. Primary measures of performance (i.e., accuracy and RT) on each of the 4 trials are provided in [supporting information \(SI\) Table S1](#). In addition, this table provides data regarding the composite measure, proactive control behavioral index.

In addition to the primary analyses, supplementary analyses were conducted to provide convergent results regarding the validity of summing the proactive control indices for RT and errors, in older adults. We conducted 2 supplemental analyses. The first involved using the approach advocated in refs. 3 and 4, in which RT and error measures are Z transformed so that they can be aggregated. Thus, for each participant, Z-score values of the error and RT index were calculated, using the mean and standard deviation for the group, collapsed across both sessions. The Z-score values were then summed to create a combined value. The results using this Z-score transformation approach replicated our results without the transformation. Specifically, following training, we observed that older adults showed increases in both the RT and error rate indices relative to pretraining performance. Each measure in isolation did not quite reach the level of statistical significance ($P_s = 0.12$ and 0.14 for error and RT, respectively). However, when the 2 measures were summed together, the effect was statistically significant: [$t(15) = -2.57, P < 0.05$].

The second supplemental analysis combined the error and RT information in terms of a speed-accuracy function, which is thought to be the gold standard for examining the rate and quality of information processing (Luce, 1986). To compute the speed-accuracy function, we binned RT into 100 msec windows, ranging from 300–1,200 msec. We then computed the cumulative accuracy for BX and AY conditions across each of the RT bins. To create a speed-accuracy function that is most similar to the proactive control index, we then computed the difference in BX vs. AY speed-accuracy function (BX-AY), which provides information about the relative advantage in processing BX vs. AY trials as a function of the latency following probe presentation. In this function, positive values reflect more accurate responses on BX trials (for which context enables unambiguous response information) relative to AY trials (for which context provides misleading response information). As can be seen in [Fig. S1A](#), older adults showed a more proactive pattern with increased BX-AY values at posttest compared with pretest. A consistent pattern was seen across all time points, with the pretest and posttest values showing significantly different ($P < 0.05$) at 900 and 1,000 msec, although the main effect of session failed to reach significance ($P = 0.11$). This confirmed our initial analyses by demonstrating an upward (more positive values) shift in the speed-accuracy function for older adults posttraining relative to pretraining. Conversely, as seen in [Fig. S1B](#), the younger adults showed the opposite pattern, a downward (more negative) shift in this function in the penalty condition relative to baseline. The baseline and penalty values were significantly different ($P < 0.05$) at 300, 400, 500, and 700 msec and showed a main effect of session (baseline vs. penalty) across all time points, $F(1, 30) = 10.16, P < 0.01$, which confirms previous findings that young adults show a behavioral pattern that is more reactive in the penalty condition.

Imaging Analyses. In [Fig. S2](#), a scatterplot is presented illustrating the correlation between the behavioral effect of strategy training in older adults (i.e., the training-related behavioral shift score) and the training effect on brain activation dynamics (i.e., the proactive control activation index). The scatterplot indicates the significant brain-behavior correlation that was observed for the left DLPFC region indicated in the main text.

In addition to the primary analyses, we conducted two addi-

tional control analyses conducted at the whole-brain level. The first was aimed to identify any regions outside of our previously defined ROIs (e.g., from ref. 6) showing a training-related proactive shift in older adults (i.e., increased cue activation at posttest, decreased probe activation at posttest). In this case, a more statistically stringent criterion was used to correct for false positives due to multiple comparisons. Thus, the following criteria were used to identify regions: (i) a significant ($P < 0.001$) session (baseline vs. posttest) by event (cue vs. probe) interaction, (ii) numerically greater cue activation in the posttest session compared with the baseline session, and (iii) numerically greater probe activation in the baseline session compared with the posttest session. Five regions were identified in this analysis, with 2 of the regions being subsets of the already identified PFC ROIs included in our primary analysis. The additional regions were also located in the frontal cortex (see [Table S2](#)).

We also conducted a parallel analysis in younger adults to identify any additional regions showing a penalty-related reactive shift. The following criteria were used to identify regions: (i) a significant ($P < 0.001$) session (baseline vs. penalty) by event (cue vs. probe) interaction, (ii) numerically greater cue activation in the baseline condition compared with the penalty condition, and (iii) numerically greater probe activation in the penalty condition compared with the baseline condition. Four regions were identified in this analysis (see [Table S3](#)). Again, most of the regions were located in the frontal cortex, but none were found to be subsets of the PFC ROIs included in primary analyses.

Together these results attest to the specificity of our ROI-based findings, and suggest that similar patterns of flexible activation dynamics were not occurring widely throughout the brain, in either perceptual and motor regions or as part of basic selective attention network.

We conducted a second supplementary imaging analysis as a negative control, to determine whether there was a separate brain network that showed robust task-related activity but which was not affected by the experimental manipulation in the same way as the PFC ROIs thought to be involved in proactive/reactive cognitive control. To test this, we identified regions showing strong event-related activation in both conditions and in both age groups, but with no effect of the experimental manipulation on activation dynamics (i.e., no differences in cue or probe activation across sessions and no overall effects of session), using a very conservative threshold. We used the following criteria: (i) significant event-related response to task trials (e.g., main effect of time, $P < 0.001$) in both the baseline and posttest sessions, (ii) no significant ($P > 0.1$) session (baseline vs. posttest) by event (cue vs. probe) interaction; and (iii) no main effect of session ($P > 0.1$). The same analyses were conducted separately in both the younger and older adult groups. We then conducted an overlap analysis to reveal only regions showing effects in both age groups.

This analysis revealed a widespread network that included both classic sensory and motor regions (such as primary visual and motor cortex), as well as components of the dorsal frontoparietal attention circuit (IPS, FEF, ACC). This network is shown in [Fig. S3](#), with classic attentional regions labeled. Again, it is important to note that these regions did show general task-related activation in both groups and in both sessions but, critically, did not show the relevant event type by session interaction, that we have taken as a marker of a cognitive control strategy shift. The activation dynamics is illustrated in a representative attentional region (bilateral FEF) for both older adults (*Top*) and younger adults (*Bottom*) ([Fig. S4](#)). This FEF region ($x = 23, y = 1, z = 51$; and $x = -22, y = -3, z = 51$) was localized according to coordinates provided in ref. 6. This result indicates that many components of the task-processing network engaged by the AX-CPT, including perceptual, motor, and attentional regions, did not show age differences or effects of the experimental manipulations. As such, these findings rule out the

hypothesis that the effects of experimental manipulations were mediated shifts in the engagement of low-level perceptual or even classic attentional processes. Most components of the task-processing network engaged by the AX-CPT, which in-

cludes not only sensorimotor, but also classic attentional regions, did not show age differences or effects of the experimental manipulations.

1. Katzman R, Brown T, Fuld P, Peck A, Schechter R, Schimmel H (1983) Validation of a short orientation-memory-concentration test of cognitive impairment. *Am J Psychiatry* 140:734–739.
2. Paxton JL, Barch DM, Storandt M, Braver TS (2006) Effects of environmental support and strategy training on older adults' use of context. *Psychol Aging* 21:499–509.
3. Salthouse TA (1992) *Mechanisms of Age-Cognition Relations in Adulthood* (Erlbaum, Hillsdale, NJ).
4. Jonides J, Marshuetz C, Smith EE, Reuter-Lorenz PA, Koeppel RA (2000) Age differences in behavior and PET activation reveal differences in interference resolution in verbal working memory. *J Cogn Neurosci* 12:188–196.
5. Paxton JL, Barch DM, Racine CA, Braver TS (2008) Cognitive control, goal maintenance, and prefrontal function in healthy aging. *Cereb Cortex* 18:1010–1028.
6. Swallow KM, Braver TS, Snyder AZ, Speer NK, Zacks JM (2003) Reliability of functional localization using fMRI. *Neuroimage* 20:1561–1577.

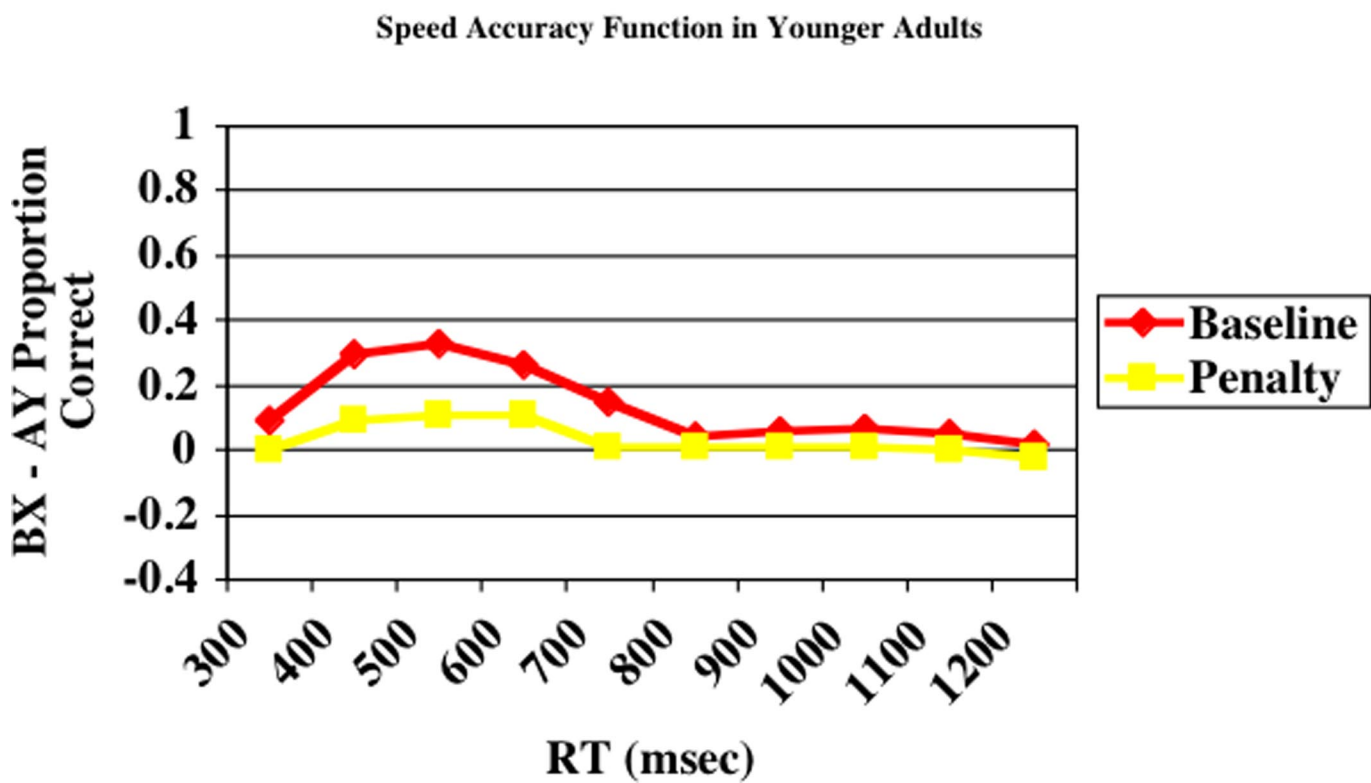
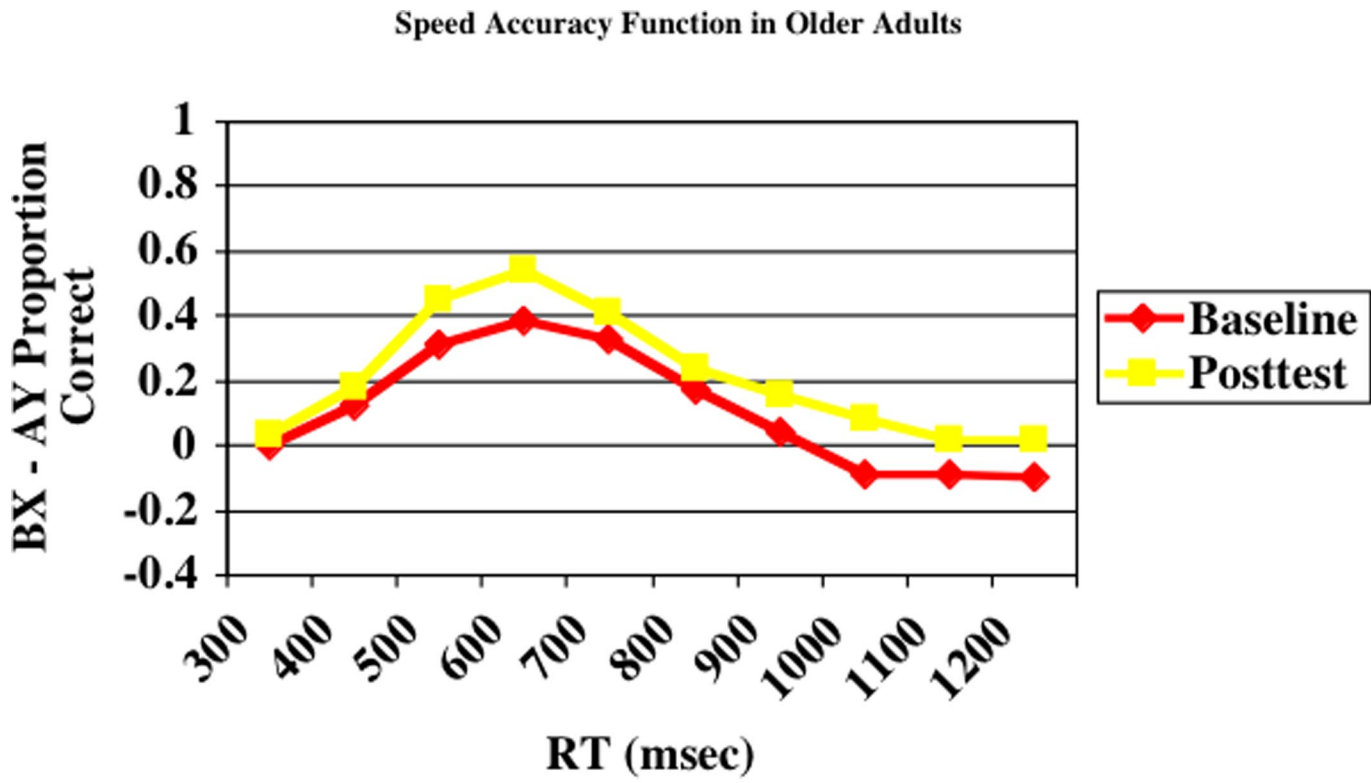


Fig. S1. (A) Speed-accuracy function of BX-AY proportion correct for baseline and posttest sessions in older adults. (B) Speed-accuracy function of BX-AY proportion correct for baseline and penalty conditions in younger adults.

Relationship between proactive shift in activation left DLPFC and proactive RT shift

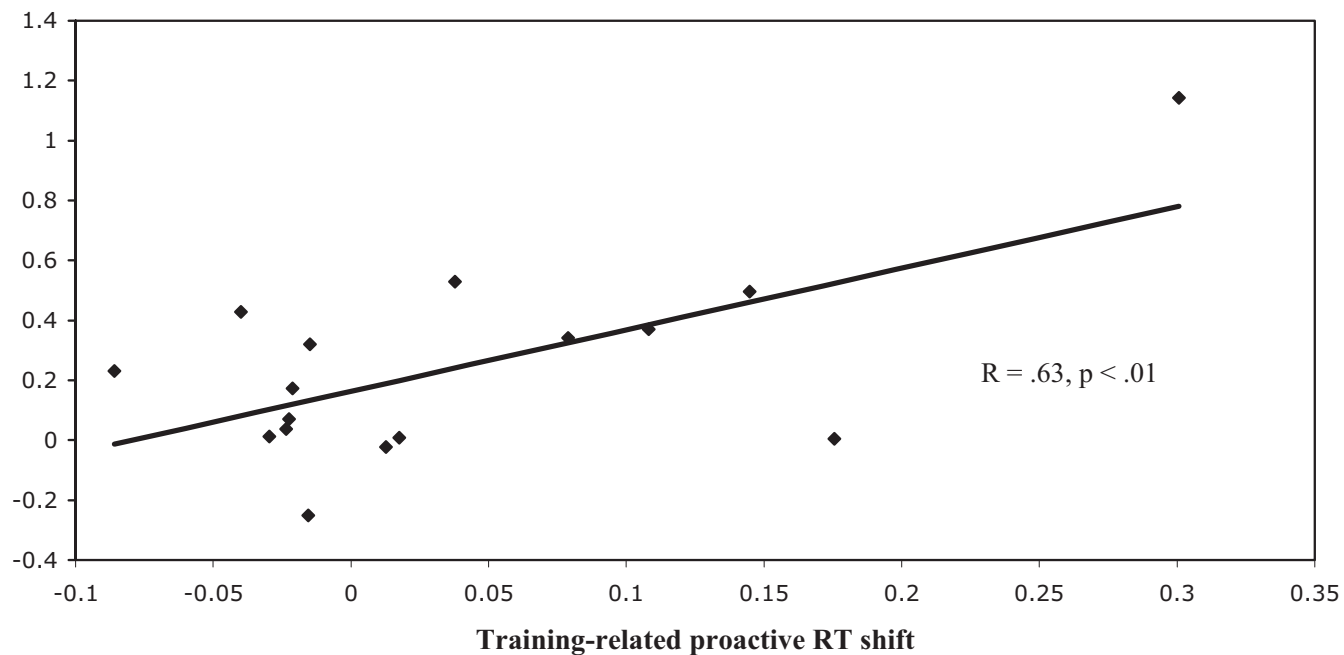


Fig. S2. Scatterplot illustrating the brain-behavior correlation in older adults within the left DLPFC ROI. The x-axis indicates the effect of training on performance, specifically the proactive shift in RT. The y-axis indicates the effect of training on activation dynamics, specifically the probe-to-cue proactive shift.

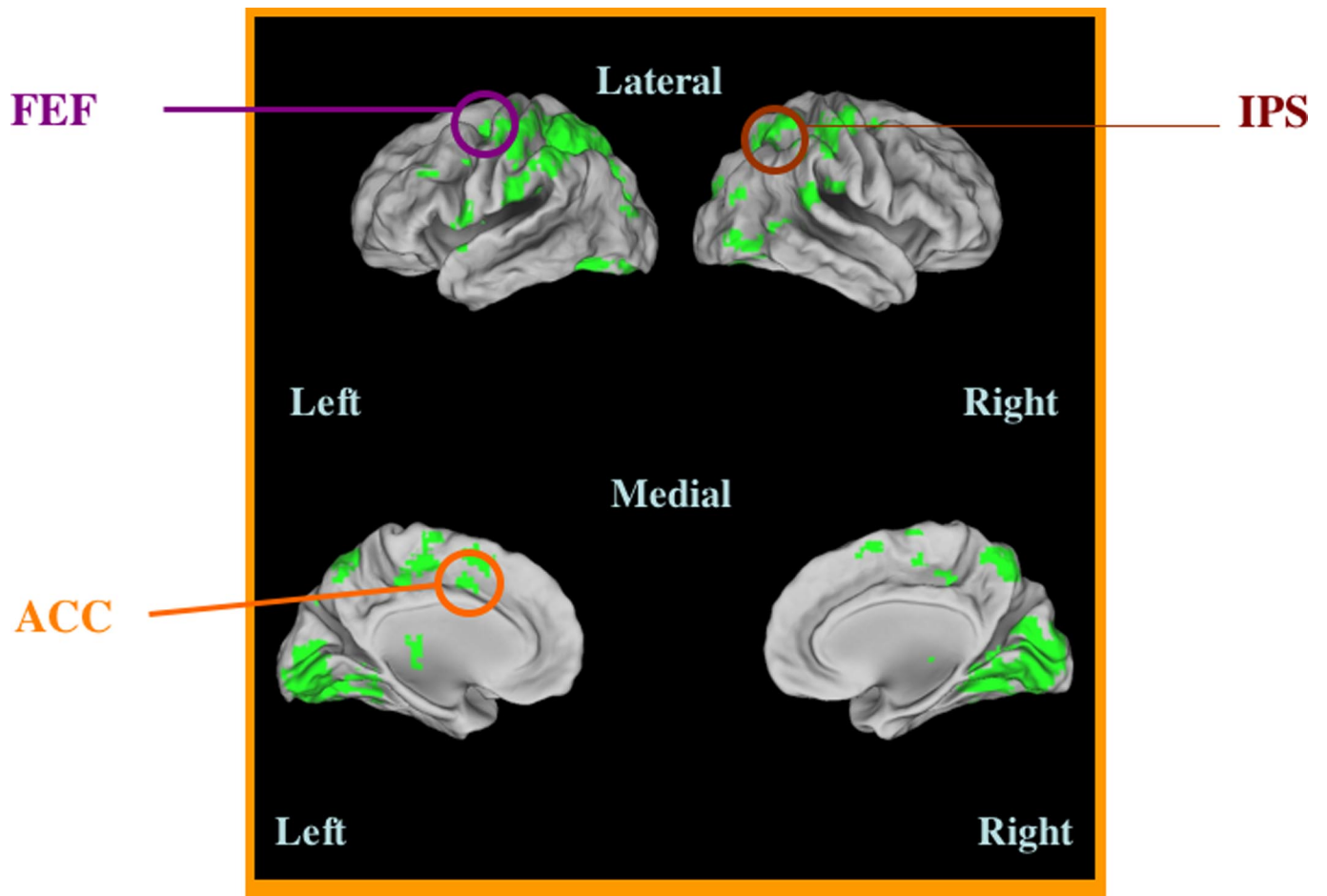
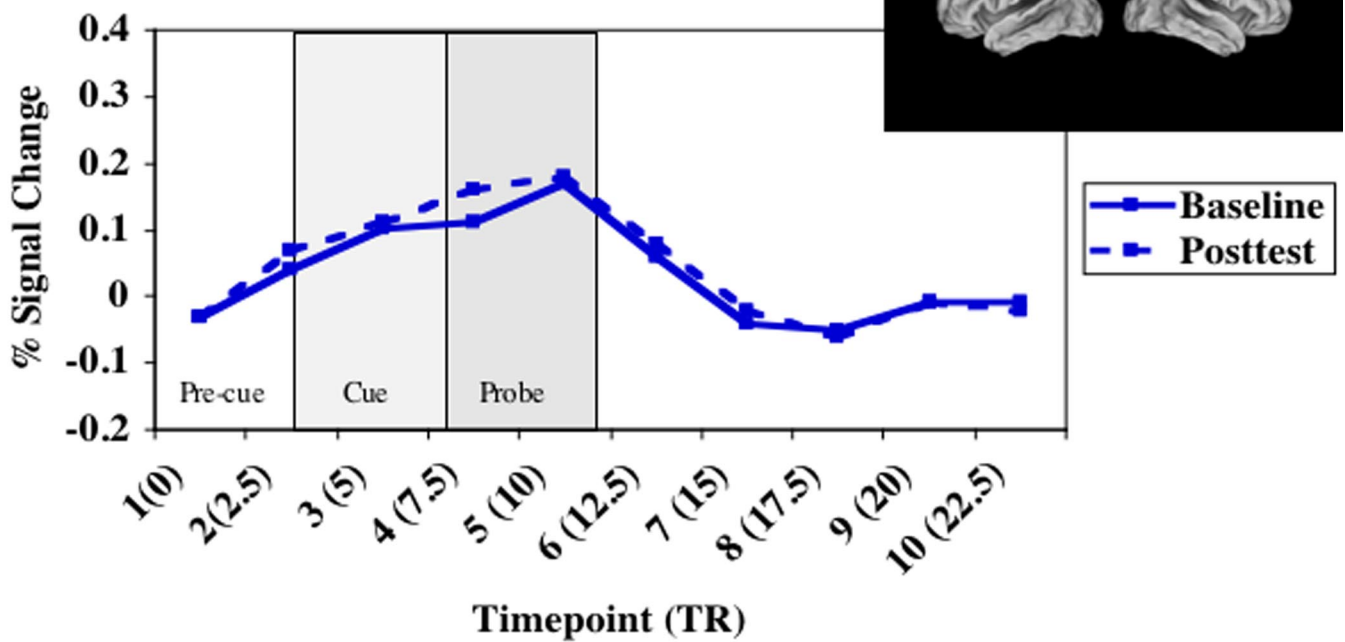


Fig. S3. Negative control regions showing task-related activity, but no effect of experimental manipulation. The *Right* side of the image is the right side of the brain, and the *Left* side of the image is the left side of the brain. Regions that are components of the dorsal frontoparietal attention circuit (e.g., IPS, FEF, ACC) are labeled.

Bilateral FEF Activation in Older Adults



Bilateral FEF Activation in Younger Adults

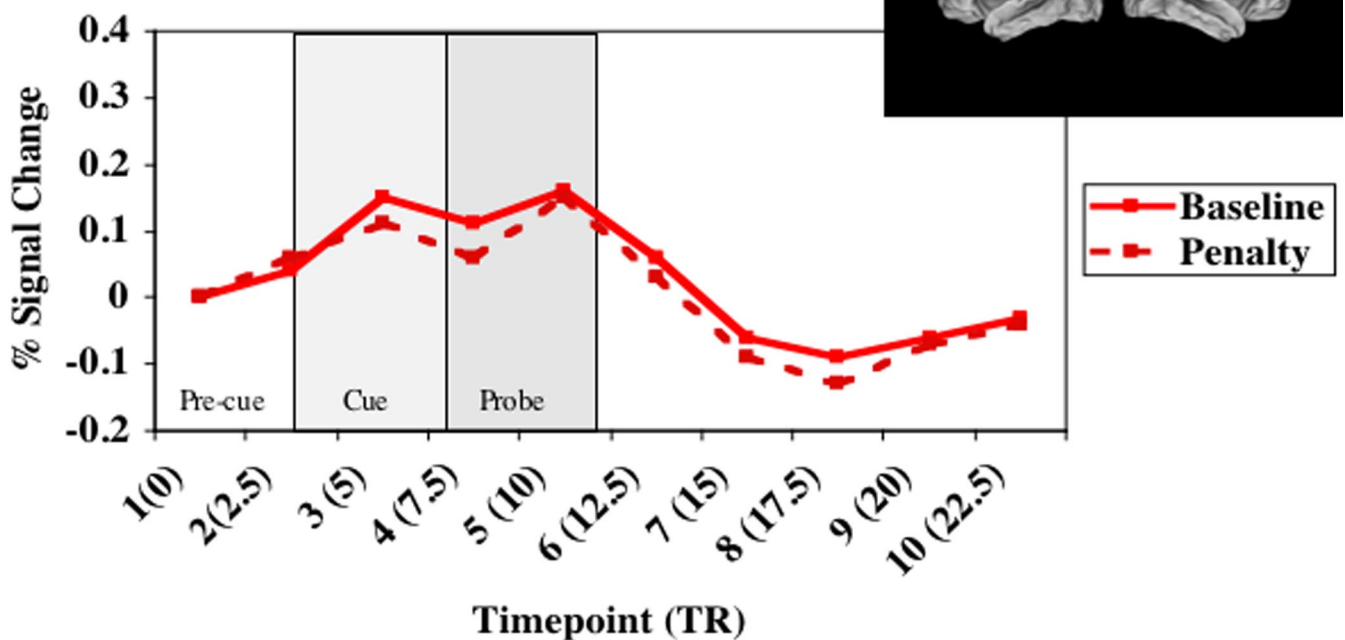


Fig. 54. Activation dynamics during trial for left ($x = -22, y = -3, z = 51$) and right ($x = 23, y = 1, z = 51$) FEF regions (activation averaged across both ROIs). *Top* image: older adults. *Bottom* image: younger adults. In both groups, there is no effect of the experimental manipulations on cue or probe activity.

Table S1. Percentage of errors and RTs in older and younger adults at baseline and after strategy training or during the penalty condition

	Older Adults		Young Adults	
	Baseline Mean (SD)	Posttest Mean (SD)	Baseline Mean (SD)	Penalty Mean (SD)
Errors				
AX	0.00 (0.01)	0.01 (0.01)	0.02 (0.03)	0.05 (0.05)
AY	0.04 (0.07)	0.06 (0.07)	0.02 (0.04)	0.03 (0.06)
BX	0.07 (0.25)	0.01 (0.03)	0.06 (0.08)	0.08 (0.10)
BY	0.01 (0.04)	0.00 (0.00)	0.01 (0.04)	0.02 (0.08)
Proactive control index	-0.01 (0.33)	0.11 (0.32)	-0.14 (0.29)	-0.17 (0.34)
RT				
AX	592 (94)	554 (116)	552 (112)	609 (150)
AY	775 (117)	760 (108)	696 (169)	704 (206)
BX	605 (159)	528 (143)	530 (182)	669 (222)
BY	610 (115)	541 (113)	547 (128)	584 (178)
Proactive control index	0.14 (0.10)	0.18 (0.12)	0.15 (0.11)	0.02**(0.04)
Sum of errors and RT				
Proactive control index	0.13 (0.39)	0.29* (0.38)	0.01 (0.28)	-0.15 (0.36)

Significant differences between sessions for proactive control index indicated in table.

* $P < 0.05$, ** $P < 0.001$.

Table S2. Regions showing training-related proactive shift in older adults as a result of whole-brain analysis

Regions of interest	Hemisphere	Brodman area(s)	X ^a	Y ^a	Z ^a	Volume (mm ³) ^b
Subgenual cingulate	Left	32	-1	32	-10	216
Inferior frontal gyrus	Right	47	52	25	0	216 ^c
Frontal operculum	Left	44/45	-37	24	7	324
Superior frontal gyrus	Left	8	-5	48	45	270
Precentral gyrus/motor cortex	Left	4	-41	-7	57	243 ^c

^aX, Y, and Z are coordinates in Talairach stereotactic space ADDIN with positive values referring to regions right of (X), anterior to (Y), and superior to (Z) the anterior commissure (AC).

^bVolume refers to the number of voxels (converted to mm³) that reached statistical significance in each region of interest.

^cRegions representing subsets of previously identified crossover regions [Paxton JL, Barch DM, Racine CA, Braver TS (2008) Cognitive control, goal maintenance, and prefrontal function in healthy aging. *Cereb Cortex* 18:1010–1028].

Table S3. Regions showing penalty-related reactive shift in young adults as a result of whole-brain analysis

Regions of interest	Hemisphere	Brodmann area(s)	X ^a	Y ^a	Z ^a	Volume, mm ^{3b}
Midbrain	Left		-4	-19	-1	243
Middle frontal gyrus	Right	9	44	2	41	243
Superior frontal gyrus	Right	6	16	-11	65	432
Superior parietal lobe	Right	7	14	-48	67	405

^aX, Y, and Z are coordinates in Talairach stereotactic space ADDIN with positive values referring to regions right of (X), anterior to (Y), and superior to (Z) the anterior commissure (AC).

^bVolume refers to the number of voxels (converted to mm³) that reached statistical significance in each region of interest.